# OBSERVATIONS AND MEASUREMENT TECHNIQUES FOR THE PASSAGE OF TURBULENT EDDIES

By

SANG GYU LIM

Bachelor of Engineering

Hanyang University

Seoul, Korea

1982

Submitted to the Faculty of the Graduate College
of the Oklahoma State University
in partial fulfillment of the requirements
for the Degree of
MASTER OF SCIENCE
December, 1983

OBSERVATIONS AND MEASUREMENT TECHNIQUES FOR

THE PASSAGE OF TURBULENT EDDIES

Thesis Approved:

P. M. Morkl
Thesis Adviser

David G. Lilley

A. J. Ghajar

Norman N. Durham
Dean of the Graduate College

ACKNOWLEDGMENTS

The author wishes to express his sincere gratitude to his major adviser, Dr. Peter M. Moretti for his wise guidance, patient advice and encouragement. He did not hesitate to discuss and give the author kind advice any time. Appreciation is also extended to other committee members, Dr. Afshin J. Ghajar and Dr. David G. Lilley.

The author would like to extend a special thank you to Dr. Lowery and Mr. Ken Pilcher. They permitted me to use the instrumental facilities and taught the author how to use them.

The author also wishes to gratefully acknowledge the Department of Mechanical Engineering for supporting the expenses for experimental equipments.

This study is dedicated to the author's parents, Mr. Byung Hee Lim and Mrs. Cheong Tae Kim, for their financial support, encouragement, and love during my study in the United States.

TABLE OF CONTENTS

TABLE

LIST OF FIGURES

## NOMENCLATURE

| | |
|---|---|
| $A_i$ | coefficients for hot-wire calibration according to King's Law ($i = 1, 2, 3$) |
| $C_D$ | pressure drag coefficient |
| D | diameter of test cylinder in cross-flow |
| d | gap between cylinder and test-section wall |
| E | voltage from voltmeter |
| f | frequency |
| H | depth of water table test section |
| h | depth of water flowing on the water table |
| Re | Reynolds number |
| S | Strouhal number |
| T | time |
| U | velocity in the x direction |
| W | width of the water table test section |
| $\psi$ | stream function |
| $\gamma$ | intermittency factor |
| $\tau$ | period |
| $\omega$ | vorticity |

Subscripts and Superscripts

| | |
|---|---|
| t | turbulent quantity |
| $\bar{}$ | time mean average |
| ' | fluctuating quantity |

# CHAPTER I

# INTRODUCTION

## I.1 The Background of Vortex Shedding

### Phenomena Behind the Bluff Body

When a flow passes bluff bodies such as cylinder, tube, bridge, or structure, there occur vortices in a periodic or sometimes complicated manner, which leads to the so-called vortex-shedding frequency. One serious structural problem should be considered when the eddy shedding frequency of the Karman Vortex Street is at or near the natural frequency of the structure.

Quantitative study started with the experiments of Strouhal and led to an empirical correlation of the periodicity f, the diameter D, the stream velocity U through the dimensionless Strouhal number S = fD/U.

In the theoretical point of view, all previous attempts seem to have been solving the Navier-Stokes equations based on the assumption of two-dimensionality in terms of stream function and vorticity.

The stream function and vorticity were defined as:

$$u = \frac{\partial \psi}{\partial y} \qquad (1.1)$$

$$v = -\frac{\partial \psi}{\partial x}$$

$$\omega = -\nabla^2 \psi \qquad (1.2)$$

Substituting these equations into the momentum equation, the governing equation can be expressed as:

$$\frac{\partial w}{\partial t} + \frac{\partial \psi}{\partial y}\frac{\partial w}{\partial x} - \frac{\partial \psi}{\partial x}\frac{\partial w}{\partial y} = \nu\left(\frac{\partial^2 w}{\partial x^2} + \frac{\partial^2 w}{\partial y^2}\right) \tag{1.3}$$

Introducing the reference length L or D and reference velocity U and $Re = UL/\nu$ or $Re = UD/\nu$, the equation (1.3) becomes:

$$\frac{\partial w}{\partial t} + \vec{\nabla} \cdot w\vec{v} = \frac{1}{Re} \nabla^2 w \tag{1.4}$$

Pearson (1) tried to solve this equation (1.4) by finite difference methods at low Reynold number, imposing the proper boundary conditions.

However, as the Reynold number increases, we cannot get the unique solution of the flow past the bluff body. This is due to the fact that if separation takes place, there will be additional shear layers whose shape and position are unknown. In other words, there is no rigorous mathematical discription to investigate the asymptotic behavior of vortex-shedding phenomena as the Reynolds number approaches infinity.

Being relatively unguided by sufficient theory, many researchers have, for the most part, resorted to the experiments and instrumentational technique making almost the same type of measurements of velocity fluctuations with respect to the Reynolds numbers and geometry.

## 1.2 Literature Survey

There has been a lot of studies (4, 5, 6, 7) about Von Karman vortex street for nearly a century. Because of the difficulties in obtaining the precise mechanism of flow separation and vortex shedding phenomena, most part of research has been done by

experimental methods rather than theoretical approaches. But some researchers demonstrated the flow pattern behind the cylinder or rectangular at the low Re number, say, Re < 100, by solving Navier-stokes equation in vorticity and stream function form using digital computers (1, 2, 3).

The vortex shedding frequencies at various Re numbers have been investigated by many authors (4, 5, 6, 7). Their results shows that there are three different ranges to be considered based on the Reynolds number: subcritical, transition, and transcritical range. And there is a supercritical range within the transition range. Figure 1 shows the vortex shedding frequencies at various Re numbers (7).

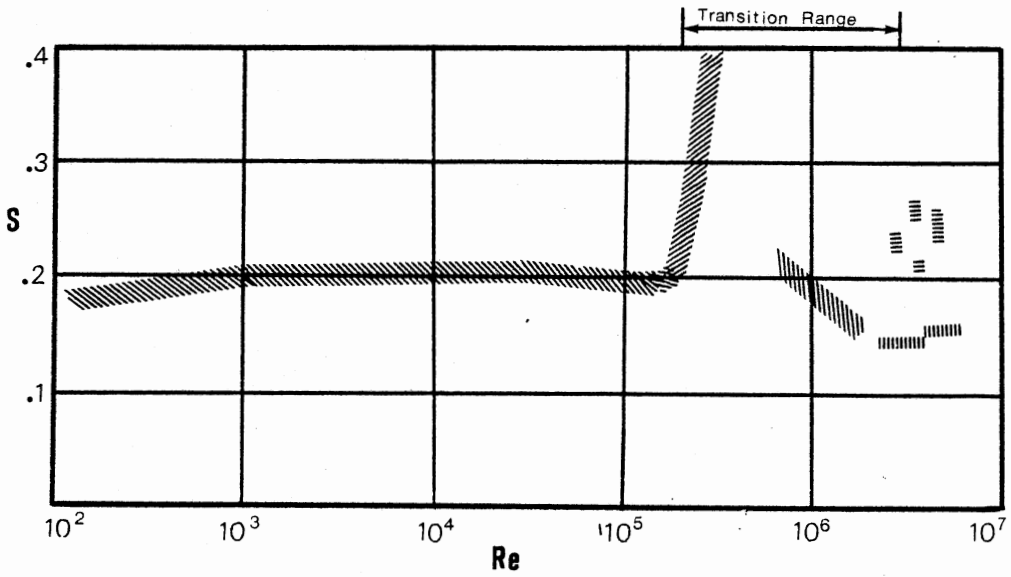


Figure 1. Strouhal Number of Vortex Shedding Frequency

In the subcritical range ($100 < Re < 2 \times 10^5$), the Strouhal number

is approximately 0.2 which is almost the same value among many authors. In the beginning of the transition range, the Strouhal number has a tendency to increase abruptly. Richter and Naudasher (6) explained this trend by the fact that because of the downstream shift of the separation lines with transition from a laminar to a turbulent boundary layer the wake is contracted.

On the other hand, the pressure drag coefficinet $C_D$ is decreased abruptly in this range. It is interesting to note that the Strouhal number is reciprocally proportional to the approximate relationship between the Strouhal number and the pressure drag coefficient by the equation (4):

$$C_D = 0.222 \frac{1}{S} - 0.0028 \frac{1}{S^2} \tag{1.5}$$

The supercritical range is characterized by the more nonlinear and irregular vortex shedding behavior and in this range the Strouhal number is going to be lower than the beginning of the transition range.

In 1961, Klebanoff et al. (8) studied this nonlinear behavior and the actual breakdown of the laminar boundary layer. An interesting behavior was drawn from their experiments that there occurred the same patterns of intense high frequency fluctuations which have something to do with the hairpin eddies. Furthermore, it was pointed out that the spikes of fluctuation occur intermittently rather than continuously, but most frequently at the spanwise position corresponding to the peak in the velocity fluctuations.

Bearman (4) studied the vortex shedding from a circular cylinder in the critical Re number range. The results reveals the fact that the reason for regular shedding ceasing is due to the increase in the three-

dimensionality of the flow caused by turbulent wedges from the front of the cylinder disrupting the separation bubbles.

Roshko (5) also explained the nature of the transitions as follows:

> At the subcritical Re numbers the separation occur early on the front of the cylinder. With increasing Re number, transition in the boundary layer moves ahead of the laminar separation point, so separation moves to the rear of the cylinder, with a consequent decrease in the drag coefficient (p. 355 )

In the transcritical range, the Strouhal numbers were lower than supercritical range, those values are somewhat scattered and there are some differences from each author.

## I.3 The Objective of this Thesis

It is well known that the dimensionless Strouhal number S is about 0.2 below the critical range. And there is a general agreement that there is, in the transition range, a predominant frequency in the wake, which leads to the irregularity and nonlinearity instead of the accurate periodicity. Furthermore, Levine (9) investigated this phenomena in the viewpoint of intermittent behavior due to large burst of turbulent fluctuations in the turbulent gas flow.

Here are two main purposes in this present study. The first one is to investigate the basic vortex shedding at the low Reynolds numbers on the water table. In this flow visualization experiment, two interesting features were focused. One of them is to get the optimum condition for flow visualization method, and the other one is to study the asymmetry effect of gap area between cylinder and the water table wall on the formation of the Von Karman vortex street.

The second objective of this thesis is to develop the method for analyzing the nonlinearity and intermittency of vortex shedding in the

beginning of the transition area by using active filters and instrumentation technique on hot-wire signals. It was hoped to obtain answeres to a few interesting and important quations: What kind of fluctuations lead to the irregularity and nonlinearity in the beginning of transition region? What is the amount of turbulent fluctuations? How does the intermittency affect the vortex shedding? Is there any quantitative characteristics in the turbulent fluctuation?

## 1.4 Outline of the Thesis

In the previous sections, the scope and objectives of this study were introduced. Various ranges of vortex shedding characteristics with respect to Reynolds number were also introduced.

Chapter II describes the flow visualization technique with dye on the water table. The main objectives of this chapter are to investigate the effect of Reynolds number and depth of water table on the condition of vortex shedding visualization and to explain the effect of asymmetry on the formation of Von Karman vortex street.

Experimental apparatus for hot-wire measurements are introduced in Chapter III. Expecially, the instrumentation procedures for detecting various signals resulted from the transition phenomena are described.

In Chapter IV, the qualitative and quantitative aspects of detected signals are explained. A separate documenation in Appendix B contains some photographs taken from the oscilloscope and spectrum analyzer. Results for Strouhal number and turbulent fluctuations are also included in this chapter.

Chapter V summarizes all of these results and suggest further research.

# CHAPTER II

# FLOW VISUALIZATION ON THE WATER TABLE

## 2.1 Experimental Arrangements

A water table of a test section 7.75 inches wide, 40 inches long and 5 inches high was used. The water was circulated by a small centrifugal pump, and the velocity in the test section was controlled by a rotometer installed at a return pipe. The schematic diagram is shown in Figure 23 (Appendix C).

In order to reduce the free-stream turbulence level, the leading edge was rounded. The vortex-shedding visualization was performed at various hights of test section. Also, the Reynolds number was dependent on the depth of the water because the flow volume was limited.

The diameters of test cylinders were from 1.3 inches to 4.5 inches. That is, the range of cylinder diameter to channel width was from 0.17 to 0.58. The dye used in developing flow-visualization was rhodamine dye.

In order to investigate the effect of asymmetry, the gap between the cylinder and the wall was varied up to one-half of the width of the test section.

In the investigation of the effect of the height in test section, the 2-inch diameter cylinder positioned 20 diameters downstream of the leading edge of the plate was used, and the velocity of water was calibrated by stop-watch.

## 2.2 The Effect of Re and Depth

In order to find the good condition for vortex-shedding visualization on the water table, this experiment was performed. The parameters included in this experiment are shown in Figure 2.

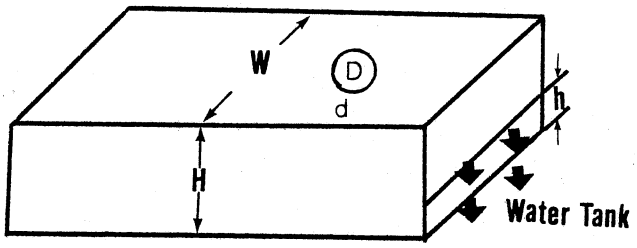


Figure 2. The Shape of Test Section of Water Table w = Width of Test Section, H = Depth of Test Section, h = the Various Depth to be Changed, D = Diameter of Test Cylinder, d = Gap Between Cylinder and Test-Section Wall

The results from this experiment are shown in Figure 3. In the effect of Reynolds and depth, h/D = 1.0 and h/D = 1.5 was perferable. Furthermore, at the Re < 2000, the visualization was good. But, the author would suggest that we can see vortex street more cleary at Reynolds number between 500 and 1000, or if possible below 500. In this case, the dye should be more light (not heavier than water). Perry et al. (19) method of visualization, or the frequency of wake was detected by a hot-wire probe or hot film.

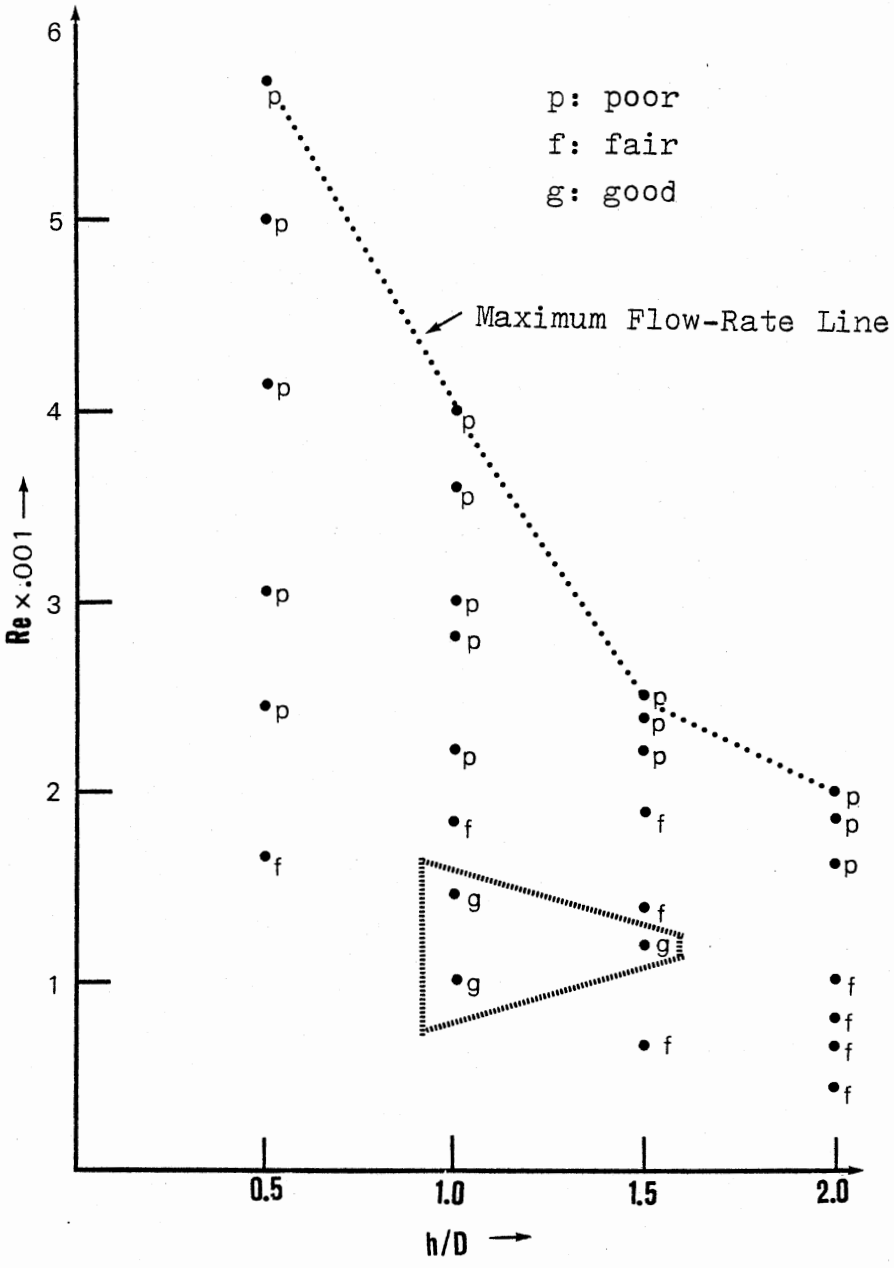


Figure 3. The Optimum Condition for Flow Visualization

## 2.3 The Effect of Asymmetry

This experiment was performed at h/D = 1.0, Re = 1000 and 5000. The diameters of test cylinders are:

$D_1$ = 1.3 in.;

$D_2$ = 2 in;

$D_3$ = 1.3 in;

$D_4$ = 3 in;

$D_5$ = 3.5 in; and

$D_6$ = 4.5 in.

In the effect of asymmetry, as shown in Figure 4, there are three regions, existence of vortex shedding, non-existence of vortex shedding and unstable (irregular) region.

At d/D = 0.1 only a single row of vortices were observed (Figure 5 [a]), but at d/D = 0.6 a regular Von Karman vortex street was seen (Figure 5[b]). At d/D = 0.3 and 0.4, there were sometimes irregular and perturbed vortex streets (Figure 5[c]). In this situation, the three-dimensional effect was also observed intermittently. This is a consequence of vortex break-down and has something to do with transition to turbulent fluctuation due to the boundary-layer effect on the wall.

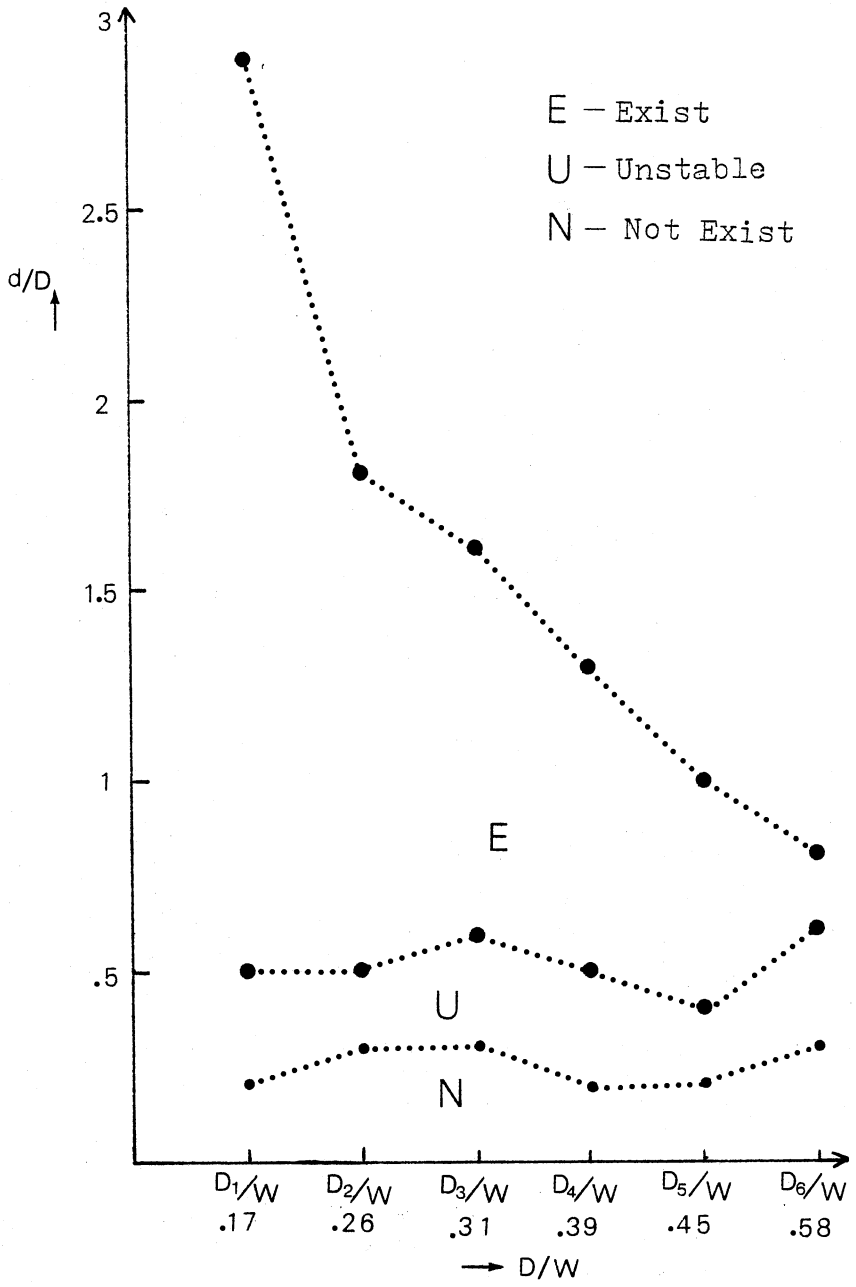


Figure 4. The Range of Vortex Shedding Existence with Respect to Gap Ratio

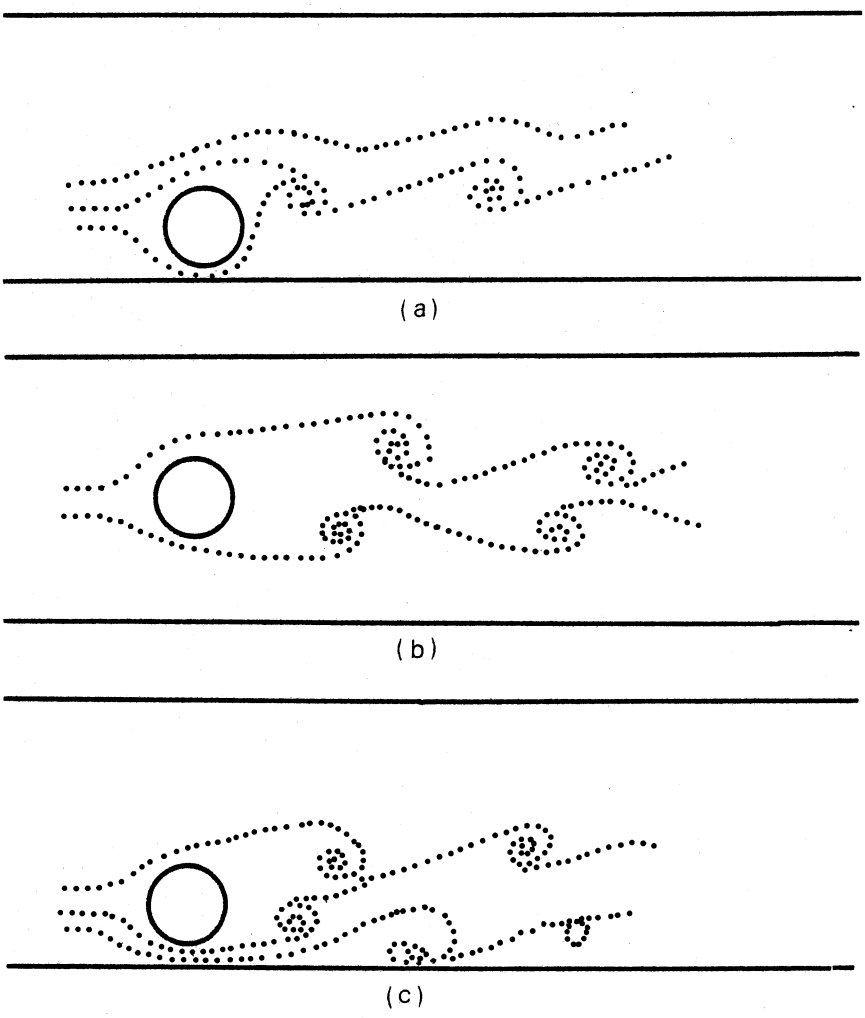


Figure 5. The Appearance of Von Karman Vortex Street

# CHAPTER III

## METHODS OF HOT-WIRE MEASUREMENTS

### 3.1 Experimental Arrangements

The experiments were performed in a high-speed wind tunnel which is located at the Mechanical Engineering Laboratory, Oklahoma State University (Figure 6).

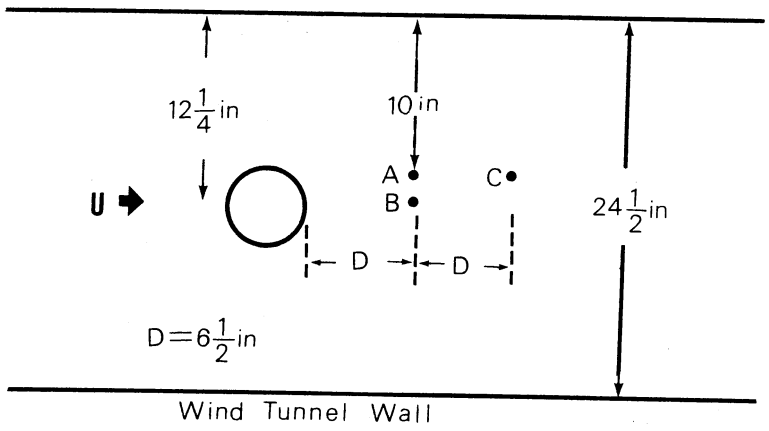


Figure 6. Arrangement of Cylinder in the Wind Tunnel

The test section of the channel was of a rectangular shape measuring 24-1/2 inches in width, 16-1/8 inches in depth and 106 inches in length. A 6-1/2 inch diameter of circular cylinder was installed in the middle of the test section and hot-wire probe was located one diameter

behind the test cylinder to measure the velocity fluctuations and vortex shedding frequencies generated by the cylinder.

The bridge is connected to the hot-wire probe, and the bridge is also connected to the oscilloscope and the spectrum analyzer. Some pictures were taken at the various situations.

## 3.2 The Free Stream Condition

The velocity was measured by DISA single type hot-wire annemometer and verified by pitot-tube measurement from velocity level 1 to 3 (Table 1).

TABLE 1

THE VELOCITY AND Re FOR EACH LEVEL

| Level | Velocity (U) | Re |
|---|---|---|
| 1 | 58 ft/sec | $1.65 \times 10^5$ |
| 2 | 73 ft/sec | $2.08 \times 10^5$ |
| 3 | 93 ft/sec | $2.65 \times 10^5$ |

The hot-wire calibration was performed based on the King's Law:

$$E^2 = A_o + A_1\sqrt{V} + A_2 V \tag{3.1}$$

After finding the coefficinets $A_o$, $A_1$, and $A_2$ by the least-square curve fitting method, the velocity was obtained by solving the quadratic equation. The intesity of the free stream turbulence was less than 0.5 percent.

The hot-wire was positioned from center to near the wall. There were some differences in r.m.s. turbulence level, however, the differences were so small that it is not necessary to account for them in this experiment. But, in order to make sure that the perturbations present were not of such a level as to introduce qualitative changes in the corresponding flow past a cylinder spanning the whole wind tunnel, a special effort was made that the test cylinder was polished smooth and a 4 mm hot-wire holder was used.

### 3.3 Instrumentational Technique for Analysis of Vortex Shedding in the Transition Region

The data recorded herein were performed at the position A in Figure 6. The velocity of free stream was 58 ft/sec and the Re number was $1.65 \times 10^5$ based on the 6.5 inch diameter. As mentioned in the introduction of this thesis, this situation is the beginning of the transition range. The typical example of recorded signal trace and the power spectra of fluctuating velocity in the wake of a circular cylinder is shown in Figure 7(a), also the pictures taken in this situation are provided in Figure 17 (Appendix B).

It is evident that the wake velocity fluctuations are composed of many sinusoidal waves, which result in a single or several sharp spectral peak at the dominant frequencies. But Figure 7(b) shows that there is no visible dominant frequency, and it leads to the following assumption that due to the large amount of turbulent fluctuation and intermittant behavior, the expected low frequency signal was swamped.

So, it is necessary to design a special filter to detect this characteristics. Figure 8 shows instrumentationl equipment and the filters

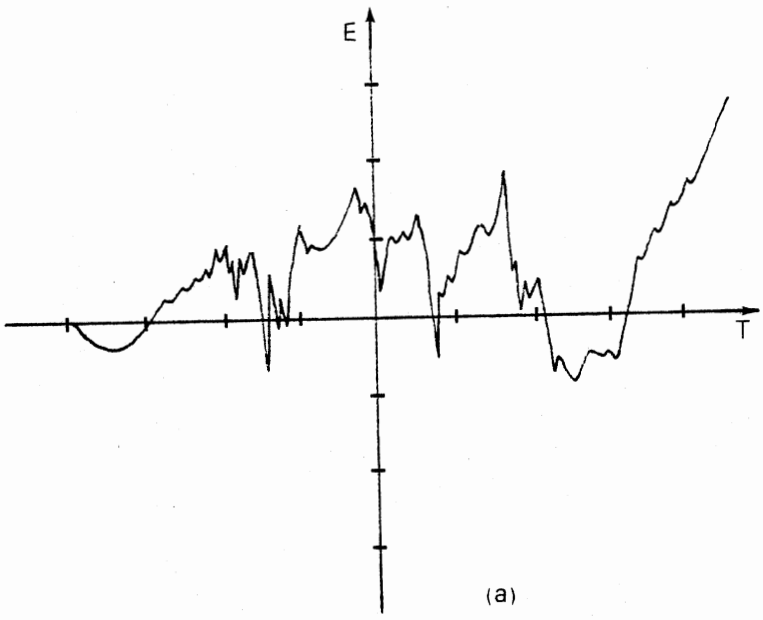


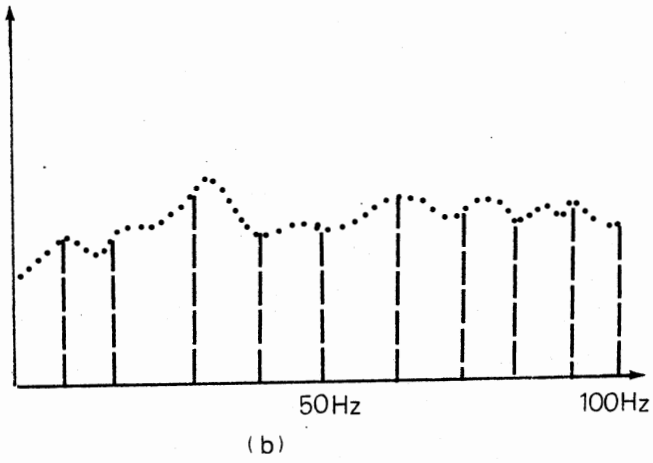


Figure 7. The Typical Example of Recorded Signal Trace and Power Spectra

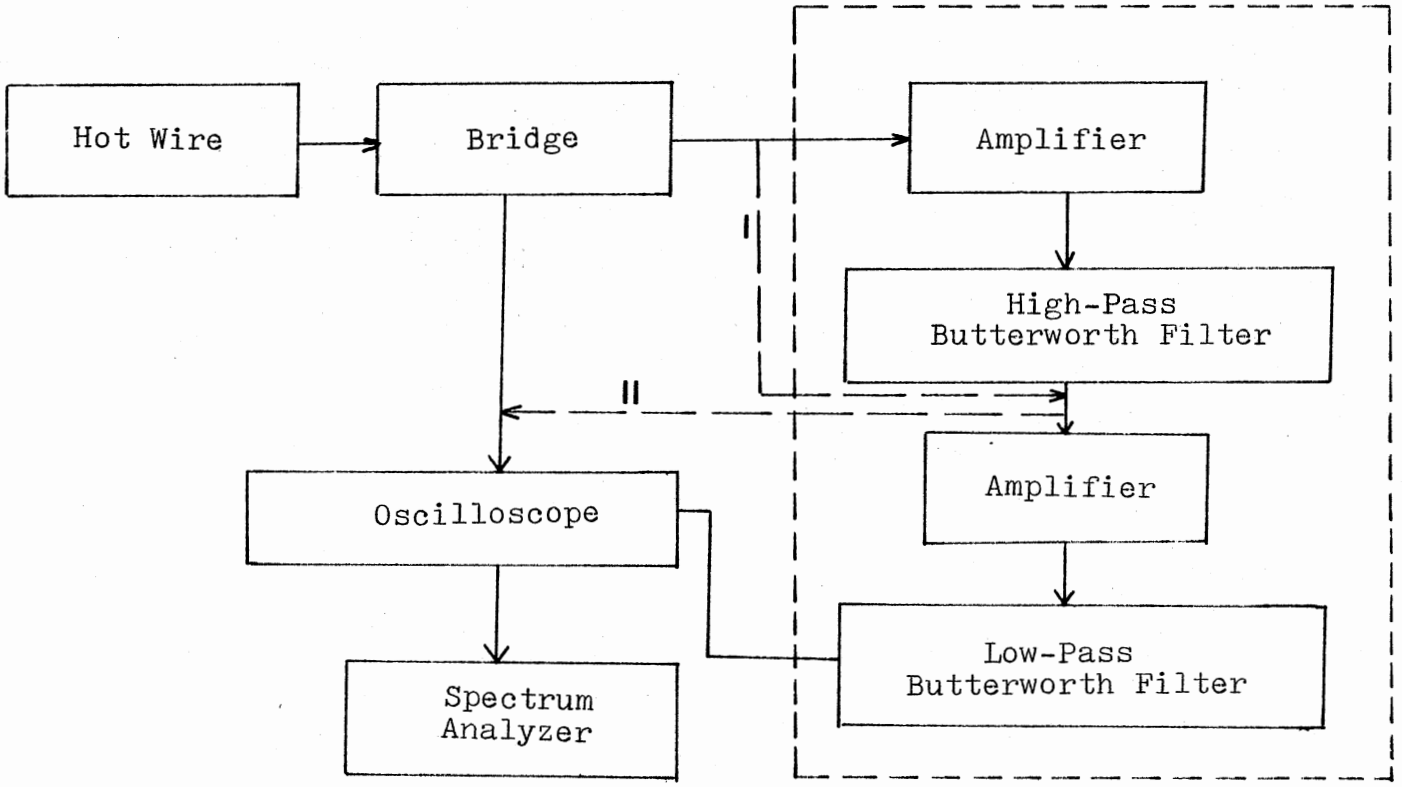


Figure 8. The Instrumental Procedure for Detecting Various Signals

to be used. According to the experiments in the wind-tunnel at position A, velocity level 1, the range of the voltage fluctuations reading from the voltmeter was approximately 0.2V. Also, it is expected that there will be some amount of voltage drop. So, two inverting amplifiers are used before the high-pass filter and low-pass filter. The detailed circuit diagram is provided in Figure 16 (Appendix A).

The cut-off frequency of the high-pass filter is 500 Hz. This filter permits of passing the intermittent turbulent high-frequency fluctuations. The typical signal passing this filter is shown in Figure 9, and the photograph is provided in Figure 18 (Appendix B).

The cut-off frequency of the low-pass filter is 200 Hz. This filter permits of passing the new low frequency signal which was resulted from the high-pass filter. That is, the high frequencies inside the period of the turbulent fluctuations were removed. The typical signal in this situation is shown in Figure 10, and the photograph is provided in Figure 19 (Appendix B).

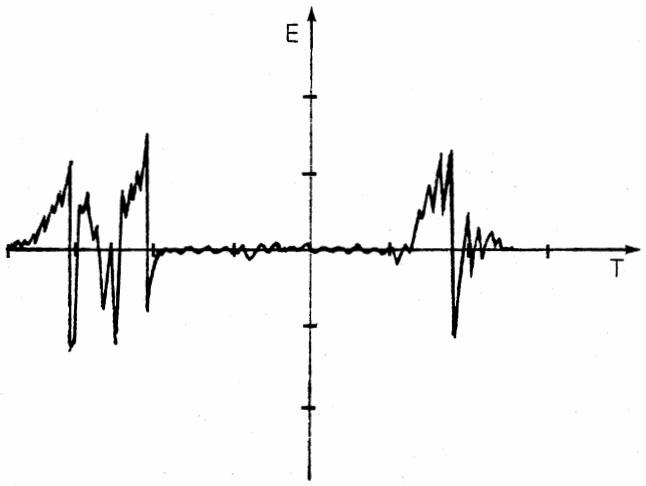


Figure 9. The Typical Signal Passed the High-Pass Filter

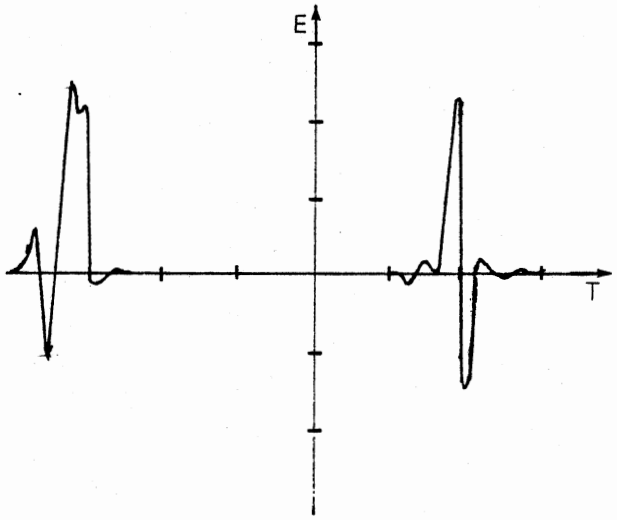


Figure 10. The Typical Signal Passed the High-Low Pass Filter

# CHAPTER IV

# ANALYSIS OF THE EFFECTS OF TURBULENT FLUCTUATIONS ON THE VORTEX SHEDDING IN THE BEGINNING OF THE TRANSITION RANGE

## 4.1 The Qualitative Aspects of the Signals

Figure 11 is an idealized signal from oscilloscope passing various path in Figure 8.

Figure 11(a) shows the original signal from the hot-wire. This is composed of three parts, the large period of fluctuations (A), the very short period of fluctuations (B), and the medium period of fluctuations which is formed by a bundle of very short period of flucuations (C).

The velocity fluctuation component U can be divided by:

$$U = \bar{U} + U' \tag{4.1}$$

where:

$\bar{U}$ = dominant velocity fluctuation; and

$U'$ = intermittant turbulent fluctuation.

It is interesting that the turbulent fluctuations have the period intermittently. Klebanoff (8) demonstrated that the intermittency occurs because the probe is sometimes inside and sometimes outside a fully developed turbulent layer. In the viewpoint of a vortex shedding behind a cylinder, the reason why we cannot obtain the regular vortex frequency

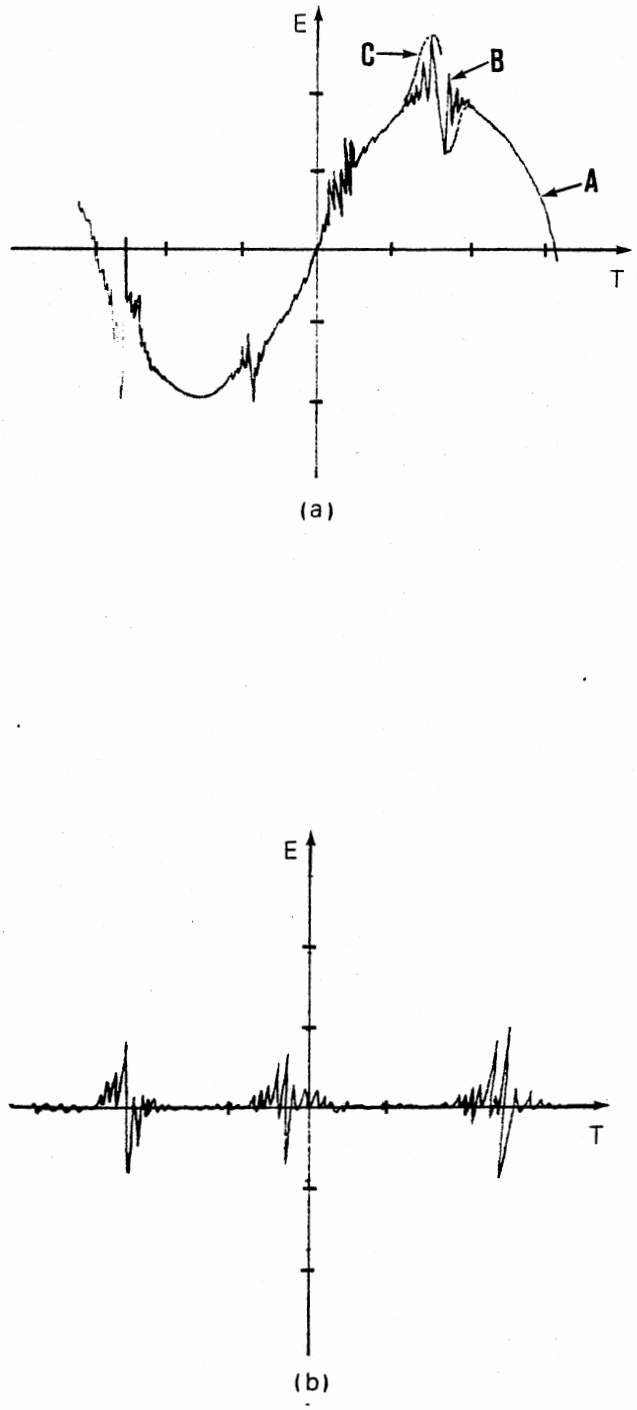


Figure 11. Idealized Signals Passing Several Paths of Instrumentation Procedure

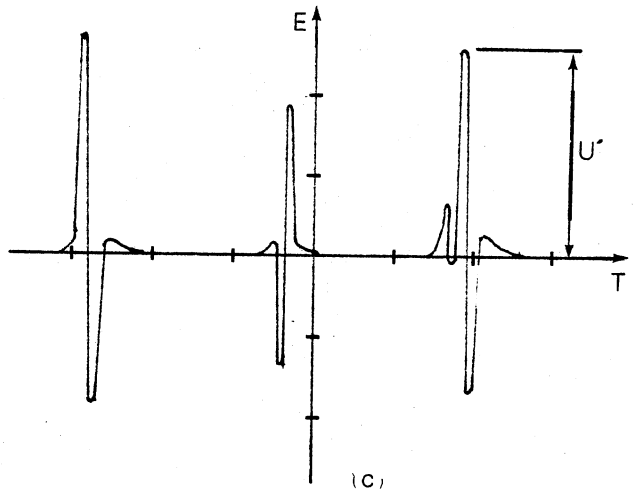


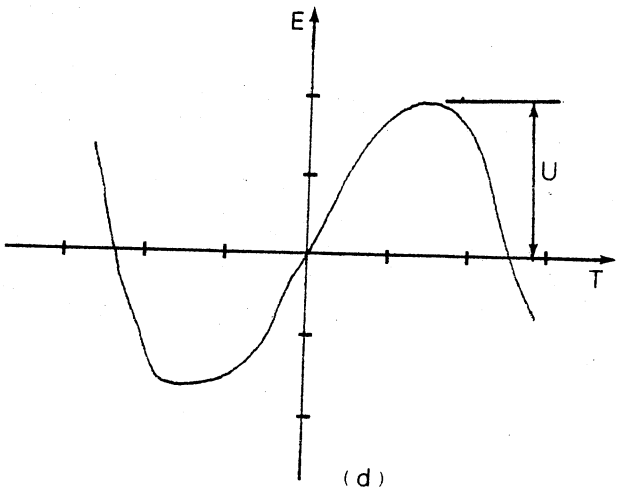


Figure 11 (continued)

is due to the fact that there occur a superposition of part (b) and part (d) in Figure 11.

The idealized signal passed only low-pass filter demonstrates the part (d) in Figure 11, of which a photograph is provided in Figure 20 (Appendix B).

One more thing to be considered at this point is the three-dimensionality. As was discussed in the flow-visualization, low-frequency irregularities are caused by the three-dimensionality. Figure 20 in Appendix B shows the low frequency irregularity, and in this experiment the three-dimensional velocity flucutation was detected by changing the hot-wire direction.

## 4.2 The Quantitative Aspects of Signals

### 4.2.1 Strouhal Number

The first one to be considered among the quantitative analysis of signals is the dominant low frequency and the value of Strouhal number. Figure 12 shows the power spectra of low frequency which passed the routine (1) in Figure 8. Namely, the intermittent turbulent behavior is removed, however, the low frequency irregularity caused by the three-dimensionality still exist. Also, the photograph taken from the spectrum analyzer is provided in Figure 21 (Appendix B).

The dominant frequency is approximately 27 Hz, and the Strouhal number is approximately 0.25, which is very similar to the value obtained by Roshko (5). The Strouhal number was also calculated by measuring the period $\tau$ from the photograph taken (Figure 20, Appendix B). The value is almost consistent with the value calculated from the power spectra.

At this point, it is worth while to introduce the effect of hot-wire

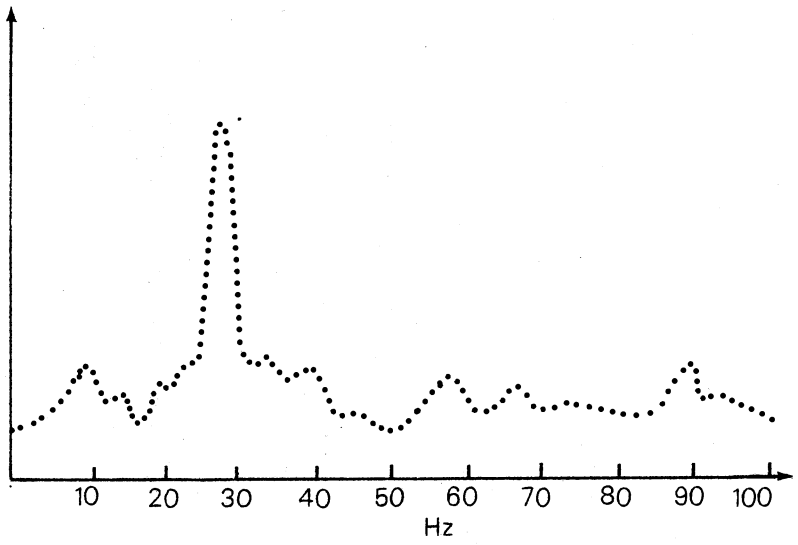


Figure 12. Power Spectra of Low Frequency

position. As the hot-wire is moved from position A to B (mean the center of wind tunnel), the amount of turbulent fluctuations are decreased, also, the intermittent phenomena are decreased. From this fact, it can be concluded that the inner part of fluctuation is more stable than outside in the transition region.

Of much importance also is the fact that the calculated Strouhal number from the low-pass filtered signal is 0.25 which is different from 0.2. This means that it proves the fact that in the beginning of the transition area, the Strouhal number has a tendency to increase as pointed out in the literature survey.

4.2.2 Turbulent Frequency

The Figure 22(a) and (b) (Appendix B) shows the original signal and low-frequency part of the turbulent signal. Susan Bloor (11) suggested the relationship between ratio of transition waves $f_t$ to fundamental shedding frequency f and Reynolds number.

$$\frac{f_t}{f} \alpha \frac{U^{2/3}}{(\nu d)^{1/2}} \frac{d}{U} = R^{1/2} \qquad (4.2)$$

Figure 13 demonstrates this relation that as the Reynolds number increases the turbulent frequency has a tendency to increase.

Another trial was made to investigate the effect of the length of downstream on the burst of turbulent fluctuations. The turbulent fluctuations at position C decreased a little bit but not much. Schaefer and Eskimazi (14) proposed the empirical relation of the stable region: the start of the stable region is governed approximately by:

$$Re(\frac{x}{d}) \doteqdot 260 \qquad (4.3)$$

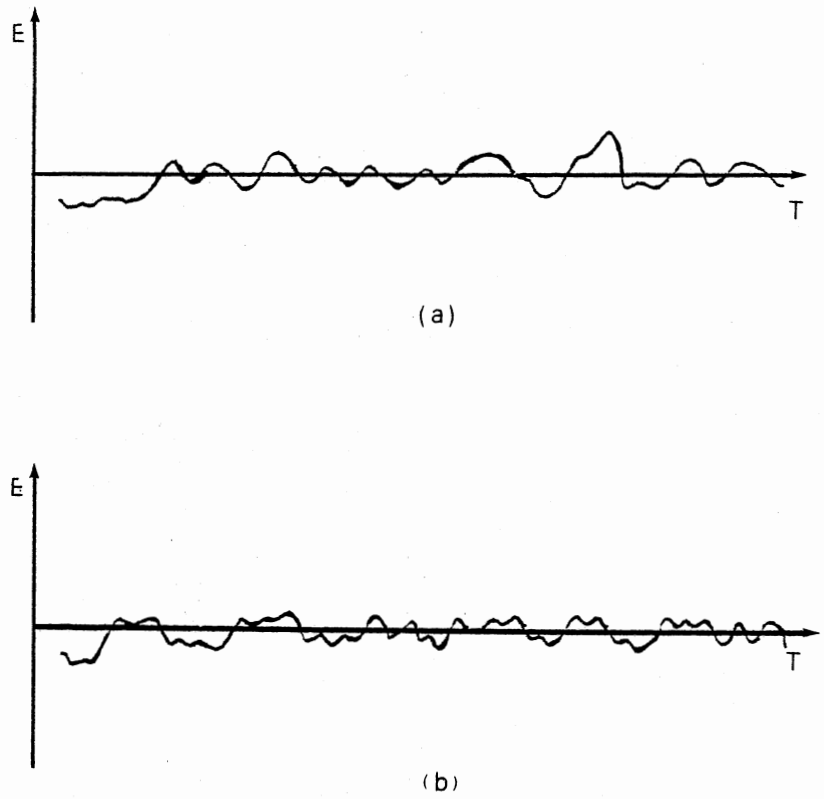


Figure 13. Low Frequency Part of the Turbulent Fluctuation. (a) Velocity Level 1. (b) Velocity Level 2

and the end of stable region is governed approximately by:

$$Re(\frac{x}{d}) \doteqdot 150 \tag{4.4}$$

where x is the length from the test cylinder to downstream location. For large Reynolds number, Equations 4.3 and 4.4 are almost meaningless. For example, if $Re = 1.6 \times 10^5$ and d = 6.5 inches, the length of stable region is approximately 0.05 inches, which is an almost meaningless value. This can be interpreted as saying that, in the transition range, the effect of the length of downstream on the vortex shedding is of little importance.

### 4.2.3 Intermittency Factor ($\gamma$)

As seen in Figure 9, the turbulent spots appears to be contained in quite sharply defined lumps or burst, instead of being uniformly distributed in time. Because the traces shown were arbitrarily selected, the number of lumps implied from the figures may not be exactly representative. However, from the statistical point of view, the intermittency factor needs to be considered.

The $\gamma$ is termed the intermittency factor (3). For $\gamma = 0$ the flow is laminar, and for $\gamma = 1$ the flow is turbulent all the time. Electronically, it is possible to obtain a measure of $\gamma$ directly from the hot-wire signal on the oscilloscope.

Figure 14 shows the simplified trace of Figure 18 (Appendix B). The intermittent turbulence is occurring about 33 percent of the time; that is, the intermittency factor $\gamma$ is equal to 0.33.

Also, the quantitative change of intermittency factor due to the movement of hot-wire from A to B is calculated. Figure 15 shows this aspect.

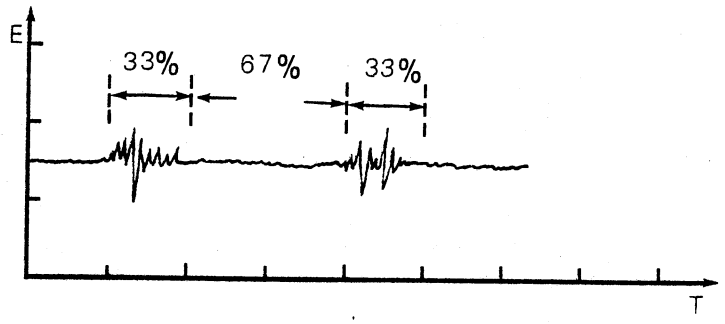


Figure 14. Trace Showing Intermittent Turbulence at Position A.

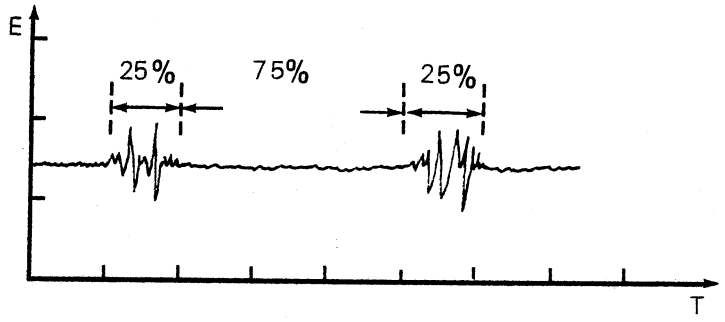


Figure 15. Trace Showing Intermittent Turbulence at Position B.

The intermittent turbulence occurring is about 25 percent of the time. That is intermittency $\gamma$ is equal to 0.25. That is, 24 percent of intermittency decrease is observed.

According to the explanation up to now, it is obvious that the reason why we cannot obtain a steady and regular vortex shedding frequency in the beginning of transition range is the interaction between low frequency and high intermittent turbulent fluctuation. Though an apparent relationship between several parameters f, $f_t$, $\gamma$, and S cannot be obtained right now, it is reasonable to guess that a superposition of low frequency and high frequency turbulent phenomena occurs; therefore, the intermittency factor is one of the important factors to be considered.

# CHAPTER V

# CLOSURE

## 5.1 Summary

This study covers development of flow visualization techniques on the water table, and the analysis of the intermittent turbulent fluctuations at the beginning of the transition range.

In the development of flow visualization techniques on the water table, the effect of the Reynolds number, the depth of water table, and the degree of asymmetry were investigated. The range of h/D for good flow visualization for the formation of Von Karman vortex street was found to be from 1.0 to 1.5 at Re $\approx$ 1000. The criterion for existence of a Von Karmon vortex street was shown to be $d/D \geq 0.5$; for $d/D \leq 0.2$ there occurred no Von Karman vortex street; and there was an unstable region $0.2 < d/D < 0.5$.

In the wind tunnel experiment at $Re = 1.65 \times 10^5$, the low-frequency fluctuation was overlaid by bursts of high-frequency turbulent fluctuations; as a result the spectral analysis did not give any explicit data.

The intermittent turbulent fluctuations, the low-frequency large fluctuation, and the low-frequency of turbulent fluctuations were detected by using active filters on the hot-wire signal. The vortex-shedding phenomena in the beginning of the transition range are characterized as the combination of these three kinds of signals.

The data from spectrum analyzer of low-pass filtered signal gave the

Strouhal number ≈0.25 for the intermittent bursts of turbulence. The intermittency factor $\gamma$ was approximately 0.33 behind the edge of the test cylinder, and 0.25 in the middle of the wake.

## 5.2 Recommendations for Future Research

The vortex-shedding phenomenon in the high Reynolds number still has uncertainties. Certainly, one of the main reasons is the introduction of the turbulent flow to the separation. The author would suggest some problems which are worthy of study:

1. In the experiment on the water table, it might be helpful to investigate the intermittency and three-dimensionality using a hot film probe because of the low Reynolds number and the possibility of visibility with naked eye.

2. The study of the effect of downstream distance of various hot-wire locations, using several hot-wires in the transtion range, is recommended.

3. The study of the effect of asymmetry on the intermittency and turbulent fluctuation in the wind tunnel is recommended.

4. If the empirical relation among the Strouhal number S, intermittency factor $\gamma$, low frequency f, high turbulent frequency $f_t$ and Reynolds number can be obtained, it will be very useful.

## REFERENCES


1. Pearson, C. E., "A Computational Method for Viscous Flow Problems." Journal of Fluid Mechanics, Vol. 21 (1965), pp. 611-622.

2. Son, J. S. and T. J. Hanratty, "Numerical Solution for the Flow Around a Cylinder at Reynolds Numbers of 40, 200, and 500." Journal of Fluid Mehcanics, Vol. 25 (1969), pp. 369-386.

3. White, F. M., Viscous Fluid Flow, McGraw-Hill, New York, 1974.

4. Bearman, P. W., "The Flow Around a Circular Cylinder in the Critical Reynolds Number Regime." Journal of Fluid Mechanics, Vol. 37 (1969), pp. 577-585.

5. Roshko, A., "Experiments on the Flow Past a Circular Cylinder at Very High Reynolds Numbers." Journal of Fluid Mechanics, Vol. 10 (1961), pp. 345-356.

6. Richer, A. and E. Naudascher, "Fluctuating Forces on a Rigid Circular Cylinder in Confined Flow." Journal of Fluid Mechanics, Vol. 78 (1976), pp. 561-576.

7. Chen, Y. N., "Properties of the Karman Vortex Street." (Lecture given at the Seminar "Vibrations Problems in Heat Exchangers" Oklahoma State University, Stillwater, OKlahoma, USA, 8th March, 1972).

8. Klebanoff, P. S., K. D. Tidstrom, and L. M. Sargent, "The Three-Dimensional Nature of Boundary-Layer Instability." Journal of Fluid Mechanics, Vol. 12 (1962), pp. 1-33.

9. Levine, A. M., V. L. Granatstein, and M. Rhinewine. "Intermittent Behavior of a Plasma Discharge in Turbulent Gas Flow." Physics of Fluids, Vol. 15, No. 12 (1972), pp. 2231-2239.

10. Alfred, A. and K. Karamcheti, "An Experiment on the Flow Past a Finite Circular Cylinder at High Subcritical and Supercritical Reynolds Numbers." Journal of Fluid Mechanics, Vol. 118 (1982), pp. 1-26.

11. Bloor, M. S., "The Transition to Turbulance in the Wake of a Circular Cylinder." Journal of Fluid Mechanics, Vol. 19 (1964), pp. 290-304.

12. Blevins, R. D., Flow-Induced Vibration, Van Nostrand Reinhold Company, New York, 1977.

13. Marris, A. W., "A Review on Vortex Streets, Periodic Wakes, and Induced Vibration Phenomena," ASME Journal of Basic Engineering, Vol. 86, 1964, pp. 185-196.

14. Schaefer, J. W. and S. Eskimazi, "An Analysis of the Vortex Street Generated in a Viscous Fluid," Journal of Fluid Mechanics, Vol. 6 (1959), pp. 241-260.

15. Iwan, W. D. and R. D. Blevins, "A Model for Vortex-Induced Oscillation of Structures." ASME Journal of Applied Mechanics, Vol. 97, 1976, pp. 19-24.

16. Morkovin, M. V., "Flow Around Circular Cylinders. A Caleidoscope of Challenging Fluid Phenomena." ASME Sympossium on Fully Separated Flows, Philadelphia, PA., 1964, pp. 102-108.

17. Rooney, D. M. and R. D. Peltzer, "Pressure and Vortex Shedding Patterns Around a Low Aspect Ratio Cylinder in a Sheared Flow at Transitional Reynolds Numbers." Transactions of the ASME, Vol. 103 (1981), pp. 88-96.

18. Bearman, P. W. and M. M. Zdravkovich, "Flow Around a Circular Cylinder Near a Plane Boundary." Journal of Fluid Mechanics, Vol. 89 (1978), pp. 33-47.

19. Perry, A. E., M. S. Chong, and T. T. Lim, "The Vortex-Shedding Process Behind Two-Dimensional Bluff Bodies." Journal of Fluid Mechanics, Vol. 116 (1982), pp. 77-90.

20. Elder, J. W., "An Experimental Investigation of Turbulent Spots and Breakdown to Turbulence." Journal of Fluid Mechanics, Vol. 9, 1960, pp. 235-246.

21. Gerrard, J. H., "An Experimental Investigation of the Oscillating Lift and Drag of a Circular Cylinder Shedding Turbulent Vortices." Journal of Fluid Mechanics, Vol. 11 (1961), pp. 244-256.

# APPENDIX A

## THE CIRCUIT DIAGRAM FOR DETECTING SIGNALS

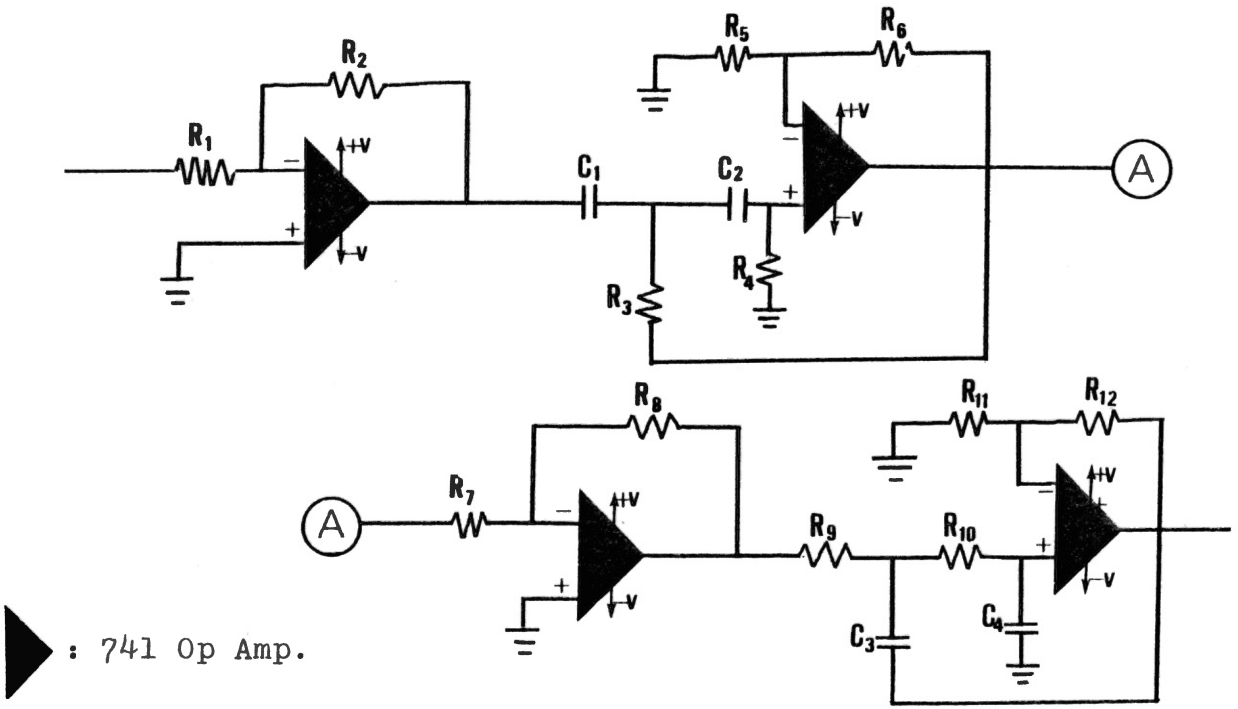


Figure 16. Detailed Circuit Diagram

# APPENDIX B

## PHOTOGRAPHS TAKEN FROM OSCILLOSCOPE AND SPECTRUM ANALYZER

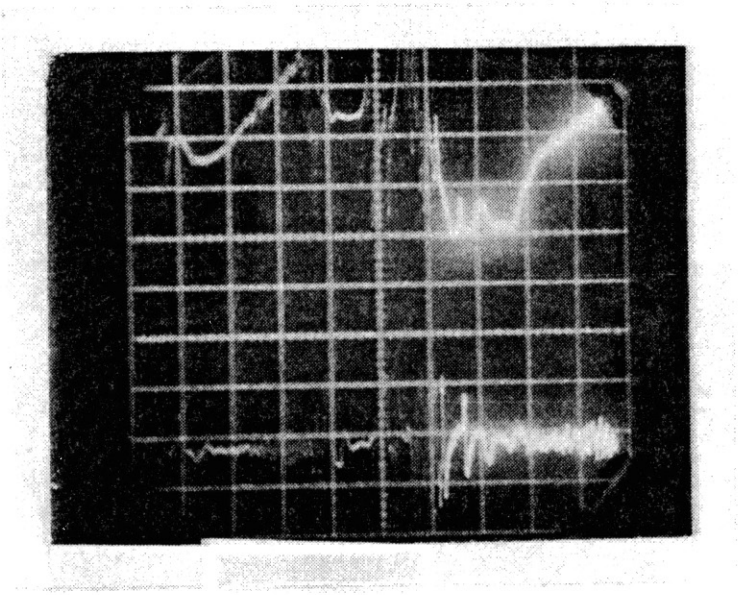

Figure 17. Photograph Corresponding to Figure 7(a)

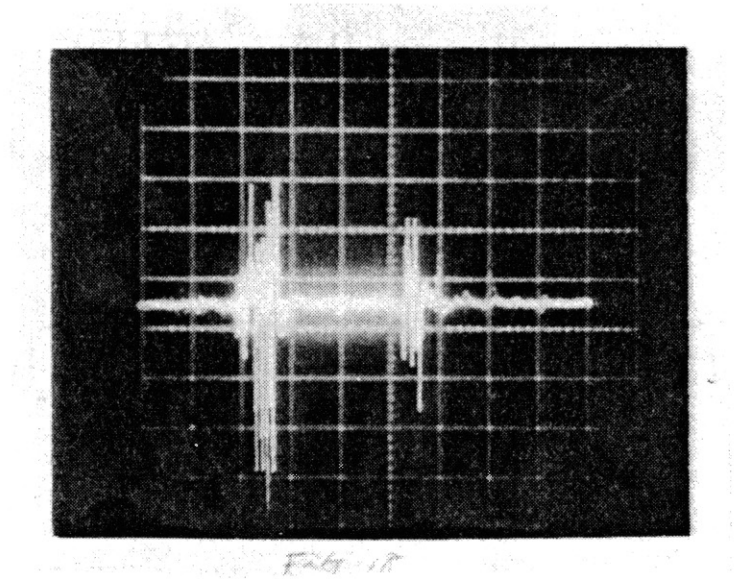

Figure 18. Photograph Corresponding to Figure 9

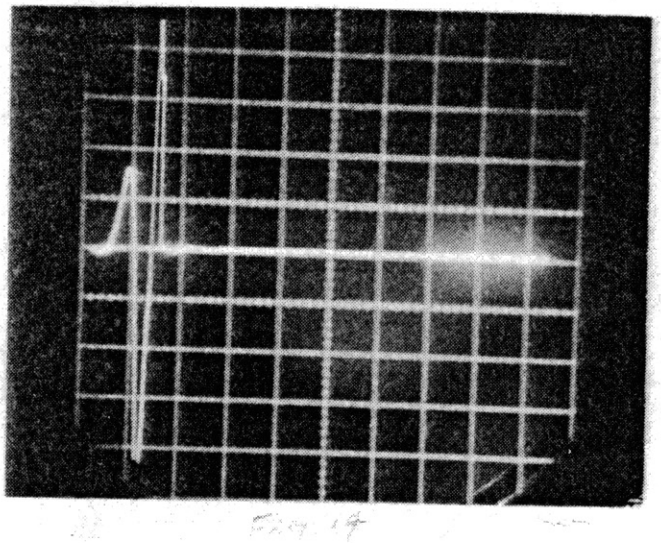

Figure 19. Photograph Corresponding to Figure 10

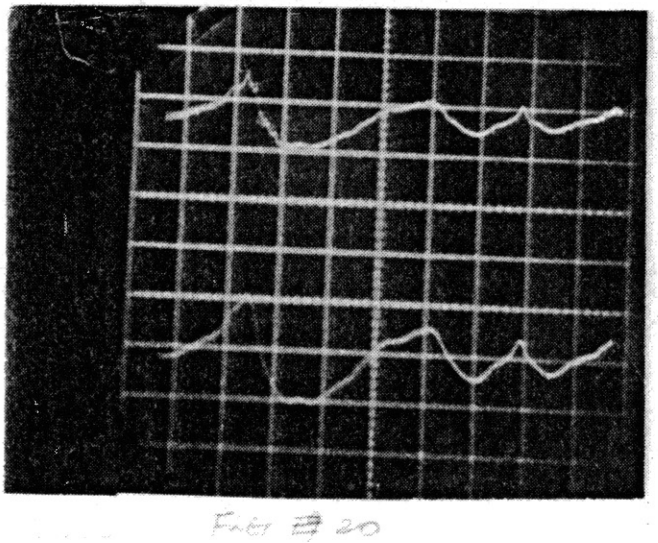

Figure 20. The Signal Trace of Low Frequency Fluctuation

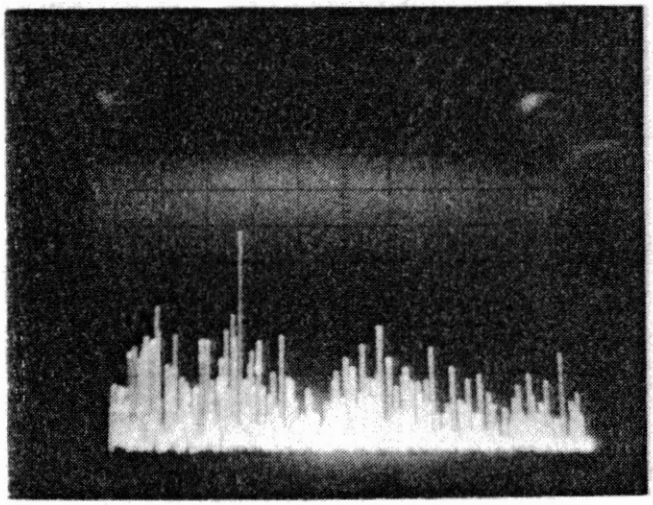

Figure 21. Photograph Corresponding to Figure 12

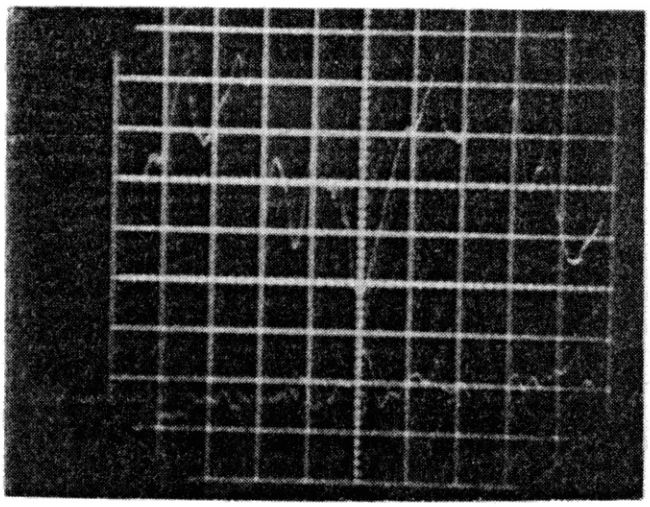

(a)

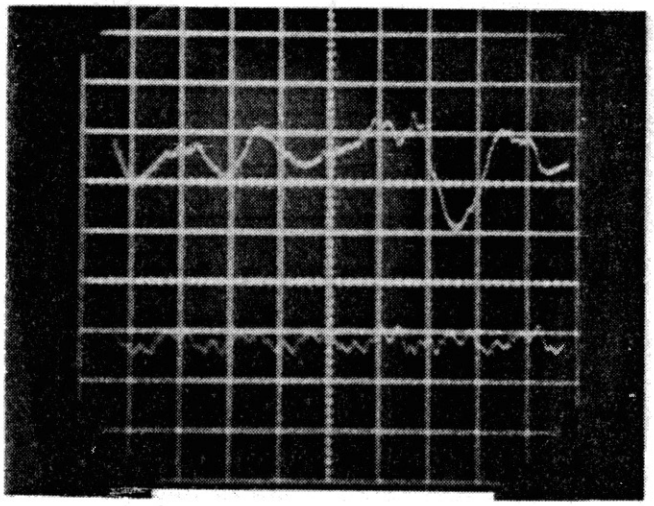

(b)

Figure 22. Photograph Corresponding to Figure 12

# APPENDIX C

## THE SCHEMATIC DIAGRAM OF WATER TABLE

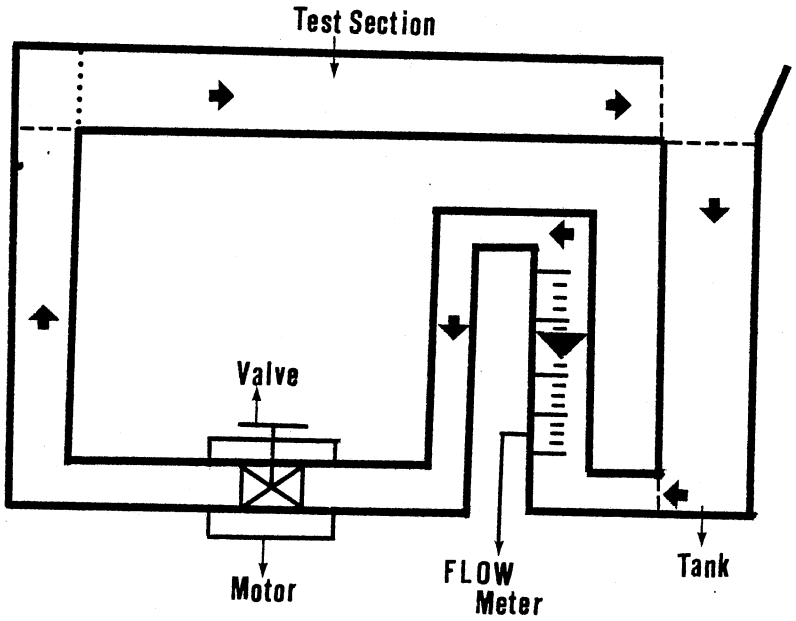


Figure 23. The Schematic Diagram of Water Table

VITA 2

Sang Gyu Lim

Candidate for the Degree of

Master of Science

Thesis: OBSERVATIONS AND MEASUREMENT TECHNIQUES FOR THE PASSAGE OF TURBULENT EDDIES

Major Field: Mechanical Engineering

Biographical:

Personal Data: Born in Kyungki-do, Korea, March 9, 1959, the son of Mr. Byung Hee Lim and Mrs. Cheong Tae Kim.

Education: Graduated from Kyung Sung High School, Seoul, Korea, in February, 1978; received Bachelor of Engineering Degree in Mechanical Engineering from Hanyang University, February, 1982; completed requirements for the degree of Master of Science in Mechanical Engineering from Oklahoma State University, December, 1983.